Related-RAS mutants identified in young-onset colorectal cancer display divergent phenotypes and retain their pro-angiogenic effects

Andrei Phillip L. David [1,‡], Mariko Isabelle P. Galvez [1,†,§], Sidney Allen A. Chua[1,§], Dominique Mickai G. Leaño[1,§], Dennis L. Sacdalan [1,2], and Reynaldo L. Garcia [1,*]

[1] Disease Molecular Biology and Epigenetics Laboratory, National Institute of Molecular Biology and Biotechnology, University of the Philippines Diliman, Quezon City 1101, Philippines; sachua@up.edu.ph, dgleano@up.edu.ph
[2] Division of Medical Oncology, Department of Medicine, University of the Philippines Manila, Manila 1000, Philippines; dlsacdalan1@up.edu.ph
‡ Present address: International Max Planck Research School for Molecular Biology, Göttingen, Germany; a.david@stud.uni-goettingen.de
† Present address: College of Medicine, University of the Philippines Manila, Manila 1000, Philippines; mpgalvez1@up.edu.ph
§ These authors contributed equally to this work.
* Correspondence: rlgarcia1@up.edu.ph

Table S1. Binding interface analysis of the AlphaFold 3-predicted RRAS-GRF1 complexes using PDBePISA.

Complex	# of interacting RRAS residues	# of interacting GRF1 residues	Binding interface area (Å^2)	ΔG_{int} (kcal/mol)	ΔG_{diss} (kcal/mol)
WT-GRF1	44	52	1719.1	-12.4	8.9
R78W-GRF1	45	52	1686.4	-12.4	12
E63D-GRF1	45	51	1757	-13	15.9

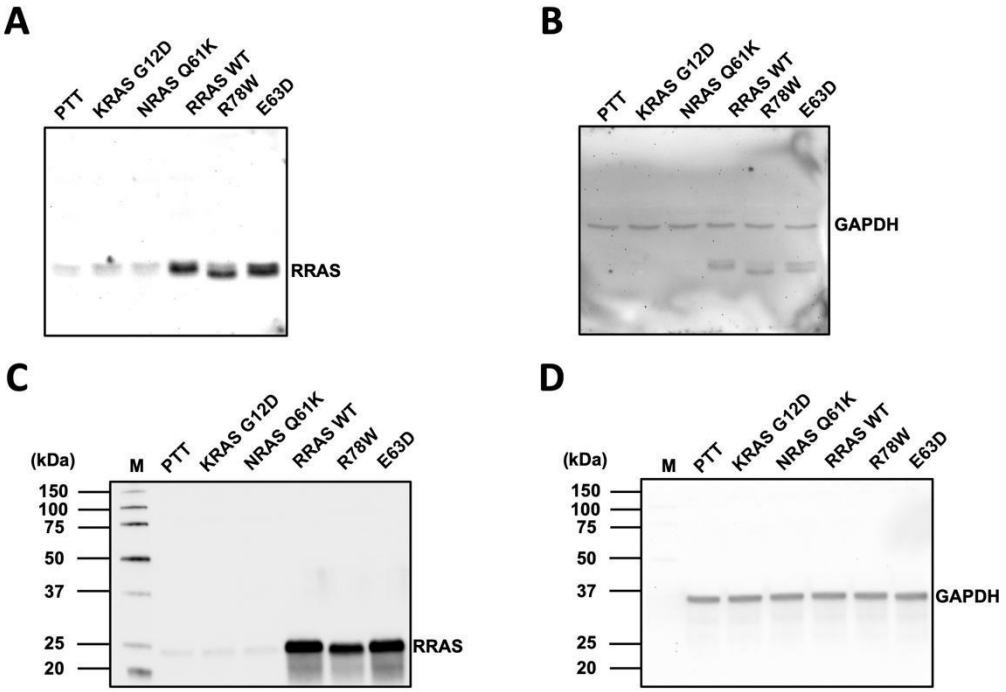


Figure S1. Western blot detection of RRAS and GAPDH in NIH3T3 and HCT116 cells. Representative blots demonstrating (**A**) RRAS and (**B**) GAPDH expression in NIH3T3 cells. Detection of (**C**) RRAS and (**D**) GAPDH in HCT116 cells transfected with RRAS mutants or controls. M: molecular weight marker; PTT: pTargeT™ empty vector; WT: wild type.

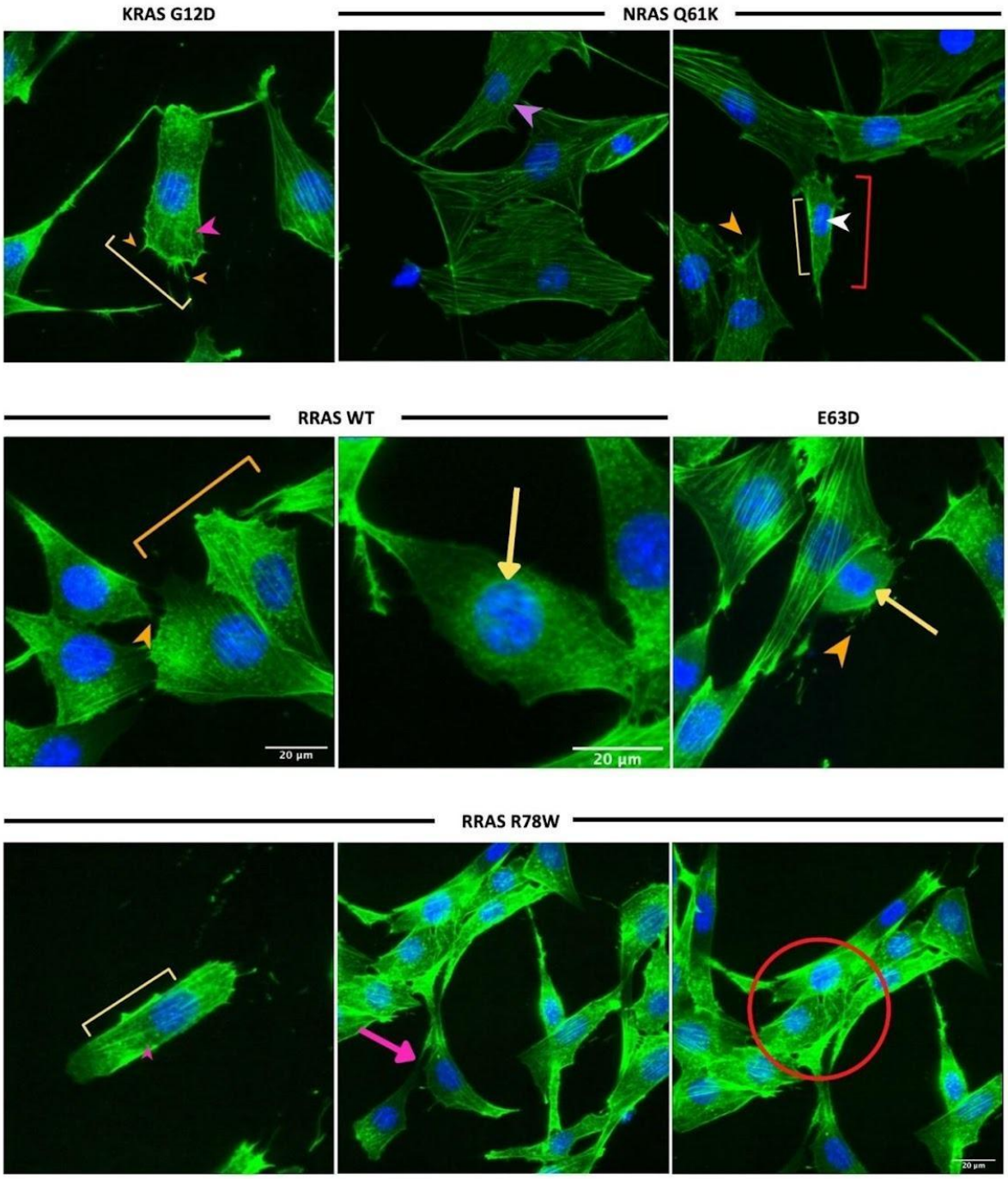


Figure S2. Enlarged images of phalloidin-stained NIH3T3 cells. Images were magnified to better visualize the cytoskeletal structures shown in Figure 1. Legend: yellow bracket: peripheral ruffles; orange bracket: lamellipodia; red bracket: shrunken cytoplasm; red circle: crisscrossing stress fibers; orange arrowhead: filopodia; white arrowhead: stretched nucleus; pink arrowhead: circular dorsal ruffles; purple arrowhead: perinuclear actin rim; pink arrow: tunneling nanotubes; yellow arrow: multilobulated cell.

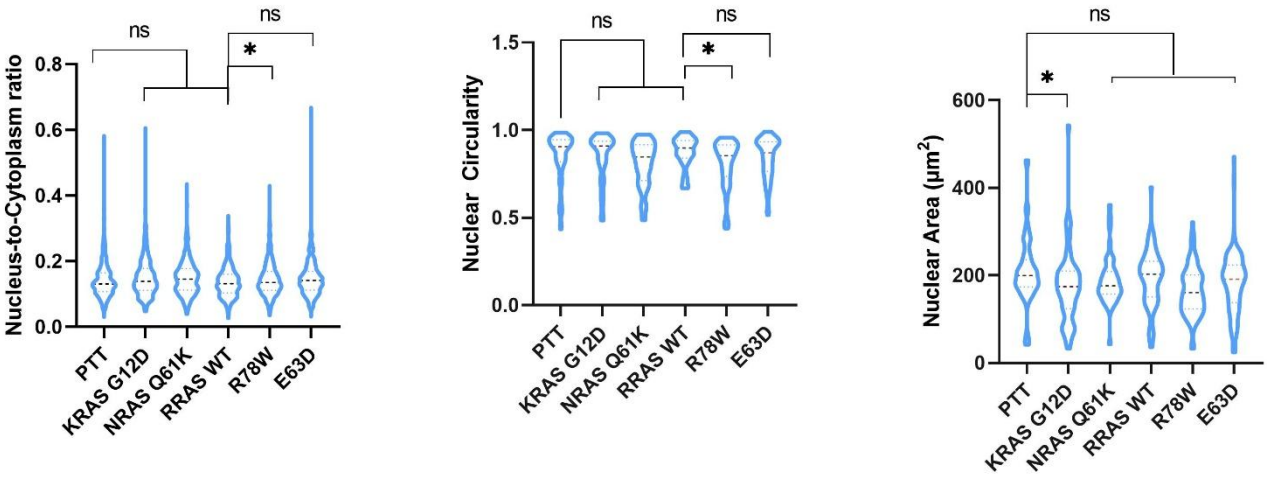


Figure S3. Cell dimensions calculated from actin staining. (**A)** Nucleus-to-cytoplasm ratio, (**B**) nuclear circularity, and (**C**) nuclear area were calculated for each of the transfected setups. *$p < 0.05$. PTT: pTargeT™ empty vector; WT: wild type.

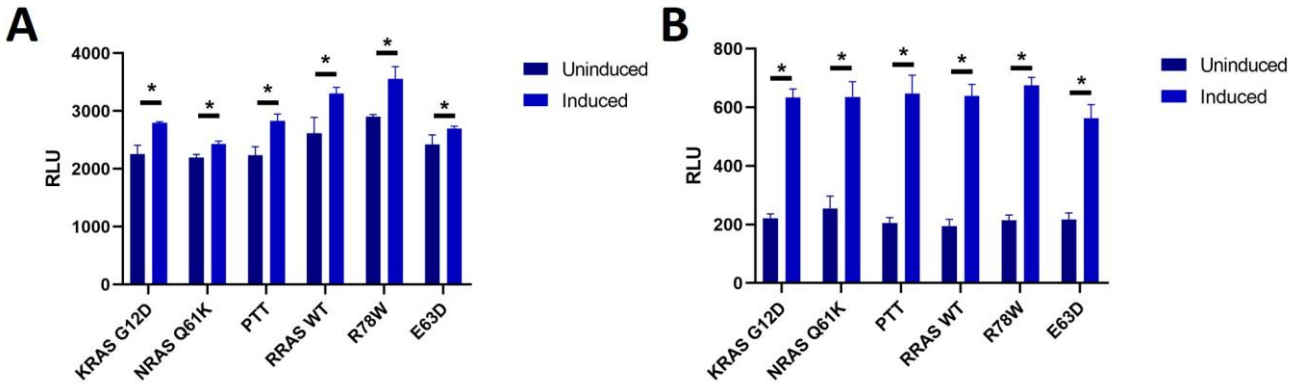


Figure S4. Apoptosis induction data for the Caspase-Glo® 3/7 Assay. Representative data for relative luminescence readings (RLU) of uninduced and induced setups done in (**A**) HCT116 and (**B**) NIH3T3 cells. Induced setups were treated with either 10mM sodium butyrate (HCT116) or serum deprivation to 0.1% NBCS (NIH3T3) for 20 hours.

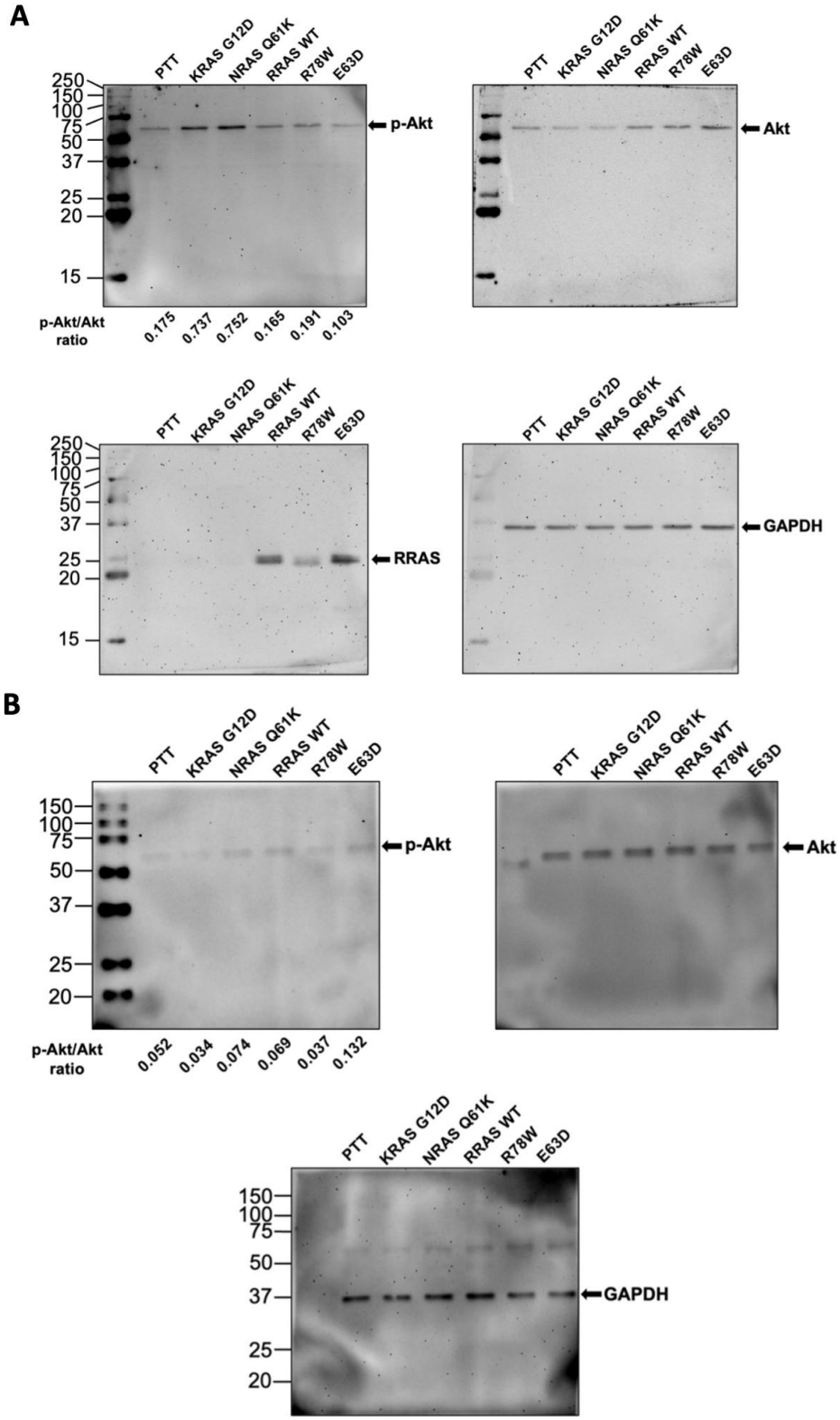


Figure S5. Western blot analysis of Akt phosphorylation in NIH3T3 cells. (**A**, **B**) Representative blots showing p-Akt and Akt expression following transfection of RRAS mutants or controls. M: molecular weight marker; PTT: pTargeT™ empty vector; WT: wild type.

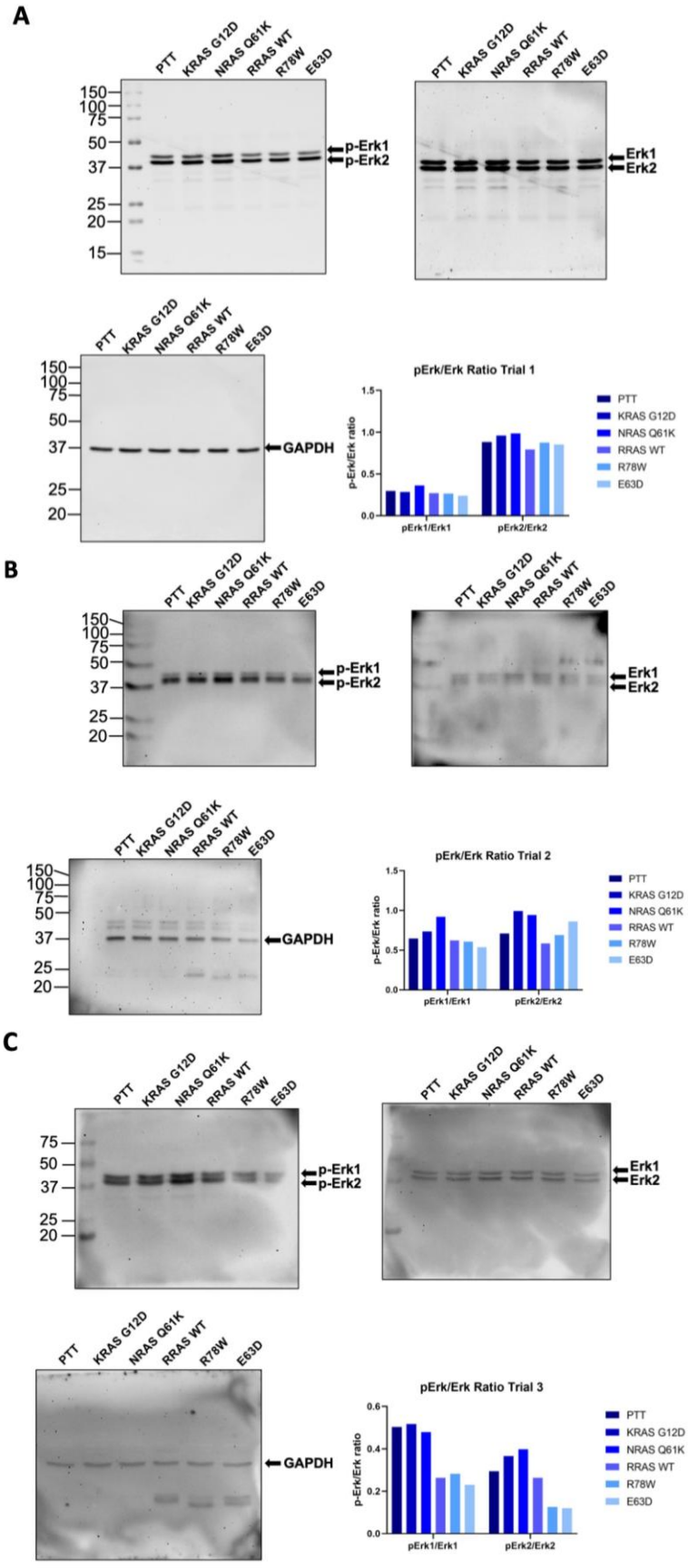


Figure S6. Western blot analysis of Erk phosphorylation in NIH3T3 cells. Representative western blot images of p-Erk and Erk expression in NIH3T3 cells transfected with RRAS mutants or controls. M: molecular weight marker; PTT: pTargeT™ empty vector; WT: wild type.

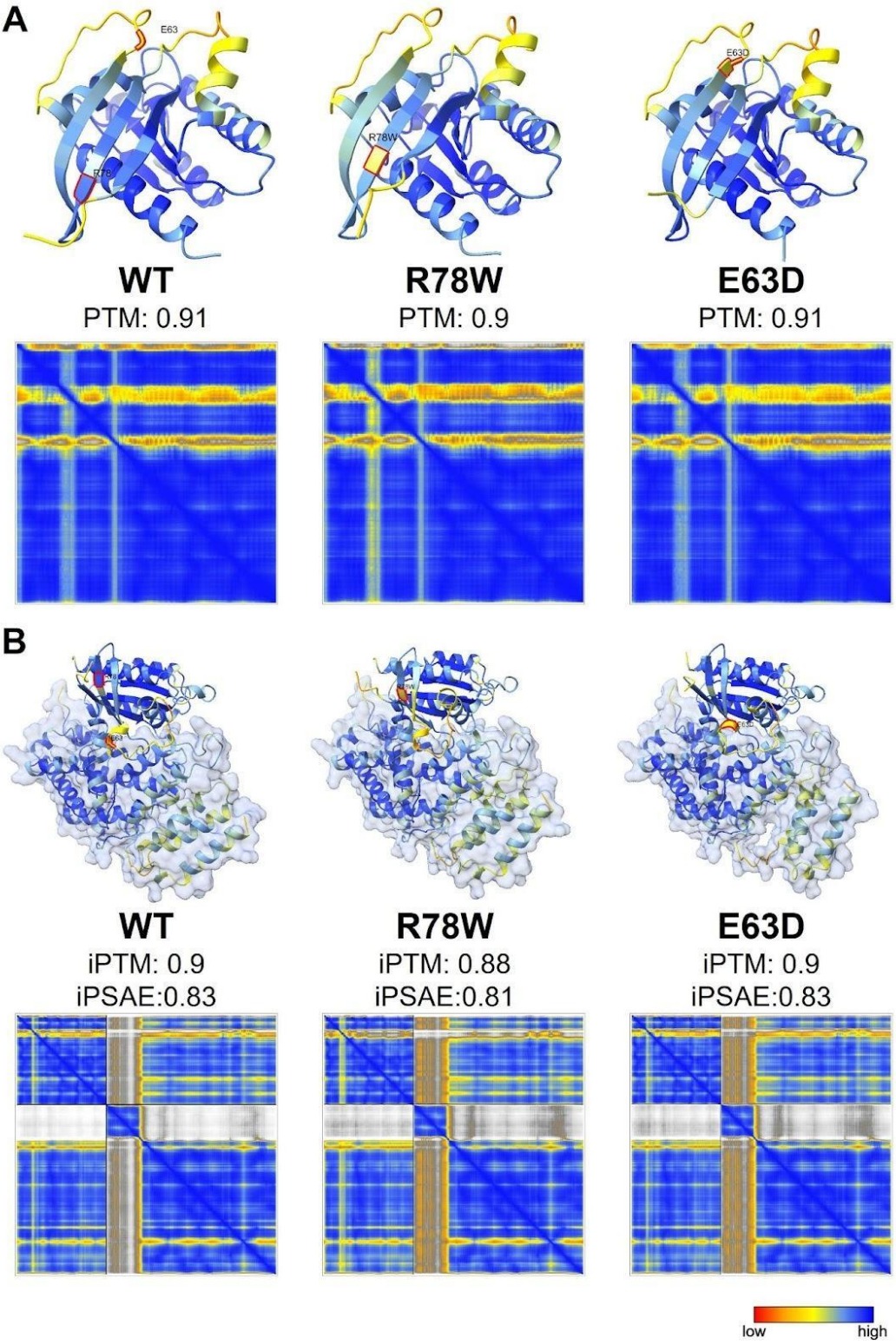


Figure S7. Confidence scores and predicted aligned error (PAE) plots of AlphaFold 3 predicted structures. (**A)** PAE plot and predicted template modeling (PTM) scores of the three predicted RRAS structures. Codons 63 and 78 are highlighted with a red outline in the wild-type (WT) structure while the corresponding mutation sites are highlighted in the E63D and R78W structures. The ribbon structures shown are color-coded based on the confidence score calculated in the PAE plot using ChimeraX. (**B)** PAE plot, interface predicted template modeling (iPTM) score, and interaction prediction score from aligned errors (iPSAE) of the prediction of the interaction between GRF1 and each of the three RRAS structures. Codons 63 and 78 were similarly highlighted with the structures in **A**. A color key for the confidence scores was generated using ChimeraX (bottom right).

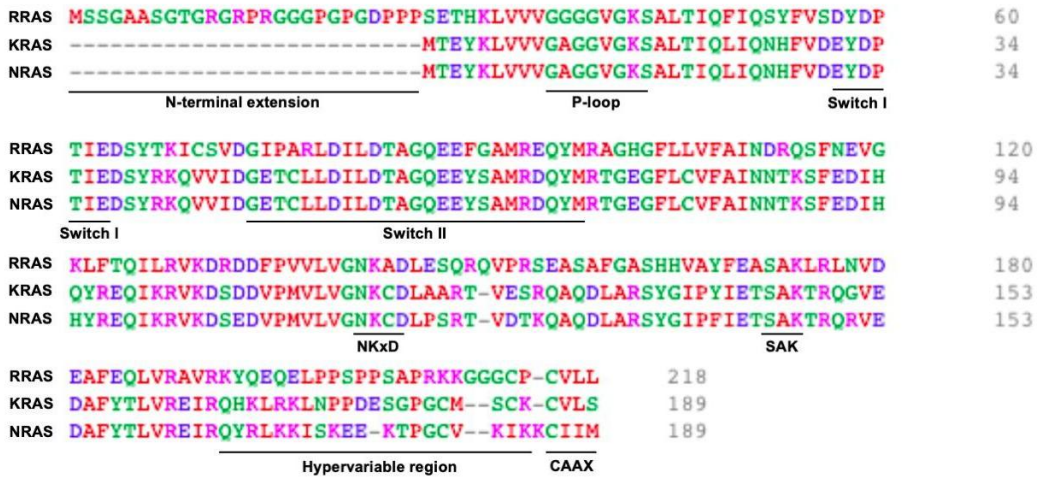


Figure S8. Multiple Sequence Alignment of the various Ras isoforms. Known conserved sequences among the Ras isoforms are highlighted using a black line.